Inorganic Chemistry

Article

pubs.acs.org/IC

Influence of the Ligand Alkyl Chain Length on the Solubility, Aqueous Speciation, and Kinetics of Substitution Reactions of Water-Soluble M_3S_4 (M = Mo, W) Clusters Bearing Hydroxyalkyl Diphosphines

Tomás F. Beltrán,[†] Rosa Llusar,*[,†] Maxim Sokolov,[†,‡] Manuel G. Basallote,*[,§] M. Jesús Fernández-Trujillo,[§] and Jose Ángel Pino-Chamorro[§]

[†]Departament de Química Física i Analítica, Universitat Jaume I, Av. Sos Baynat s/n, 12071 Castelló, Spain

[‡]Nikolaev Institute of Inorganic Chemistry, SB RAS, Prospekt Lavrentyeva 3, 630090 Novosibirsk, Rússia

[§]Departamento de Ciencia de los Materiales e Ingeniería Metalúrgica y Química Inorgánica, Facultad de Ciencias, Universidad de Cádiz, Apartado 40, Puerto Real, 11510 Cádiz, Spain

Supporting Information

ABSTRACT: Water-soluble $[M_3S_4X_3(dhbupe)_3]^+$ diphosphino complexes (dhbupe = 1,2-bis(bis(hydroxybutyl)phosphino)ethane), $\mathbf{1}^+$ (M = Mo, X = Cl) and $\mathbf{2}^+$ (M = W; X = Br), have been synthesized by extending the procedure used for the preparation of their hydroxypropyl analogues by reaction of the $M_3S_4(PPh_3)_3X_4(solvent)_x$ molecular clusters with the corresponding 1,2-bis-(bishydroxyalkyl)diphosphine. The solid state structure of the $[M_3S_4X_3(dhbupe)_3]^+$ cation possesses a C_3 symmetry with a cuboidal M_3S_4 unit, and the outer positions are occupied by one halogen and two phosphorus atoms of the diphosphine ligand. At a basic pH, the halide ligands are substituted by hydroxo groups to afford the corresponding $[Mo_3S_4(OH)_3(dhbupe)_3]^+$ ($\mathbf{1}_{OH}^+$) and $[W_3S_4(OH)_3(dhbupe)_3]^+$ ($\mathbf{2}_{OH}^+$) complexes. This behavior is similar to that found in 1,2-bis(bis(hydroxymethyl)phosphino)ethane (dhmpe) complexes and differs from that observed for 1,2-bis(bis(hydroxypropyl)phosphino)ethane (dhprpe) derivatives. In the latter case, an alkylhydroxo group of the functionalized diphosphine replaces the chlorine ligands to afford Mo_3S_4 complexes in which the deprotonated dhprpe acts in a tridentate fashion. Detailed studies based on stopped-flow, $^{31}P\{^1H\}$ NMR, and electrospray ionization mass spectrometry techniques have been carried out in order to understand the solution behavior and kinetics of interconversion between the different species formed in solution: **1** and $\mathbf{1}_{OH}^+$ or **2** and $\mathbf{2}_{OH}^+$. On the basis of the kinetic results, a mechanism with two parallel reaction pathways involving water and OH^- attacks is proposed for the formal substitution of halides by hydroxo ligands. On the other hand, reaction of the hydroxo clusters with HX acids occurs with protonation of the OH^- ligands followed by substitution of coordinated water by X^-.

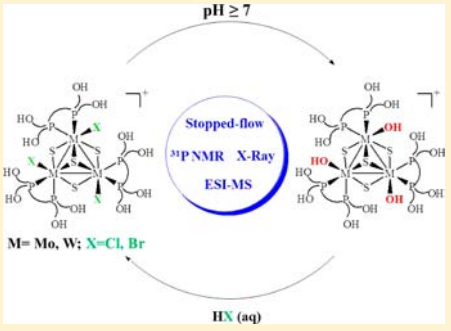

INTRODUCTION

Catalyst development aimed at constraining the metal complex to the aqueous phase of a biphasic process is mostly based on the coordination of hydrophilic ligands to an active metal center.[1] In general, chemical functionalities are introduced into the ligands of a known catalyst in order to preserve the electronic and steric properties that provide stability, activity, and selectivity to the system. In the case of phosphines, ionic functionalities are the most widely used water solubilizing hydrophilic substituents, although nonionic groups such as polyols have also been employed.[2,3]

Cuboidal clusters containing M_3S_4 (M = Mo, W) units have received long-term attention due to their potential as metalloligands in front of a second transition metal M′ to yield cubane-type $M_3M'S_4$ clusters that share similarities with some biological catalytic active sites.[4] Catalytic activity based on the heteroatoms has been demonstrated.[5] Most recently, cuboidal molybdenum and tungsten trimetallic M_3S_4 hydride clusters containing diphosphine ligands have been shown to be efficient catalysts for the regioselective defluorination of pentafluoropyridine at the 4-position.[6] Catalytic activity is higher for the tungsten complexes with turnover numbers close to 100, whereas reactions catalyzed by molybdenum are faster. Furthermore, the molybdenum hydride complexes have also shown an unprecedented catalytic activity for the selective reduction of nitrobenzene derivatives to anilines with almost quantitative conversions and yields.[7] On the other hand, incomplete cubane-type $Mo_3S_4^{4+}$ aquo clusters supported on a highly oriented pyrolitic graphite possess a high electrocatalytic

Received: April 11, 2013
Revised: June 21, 2013
Accepted: July 2, 2013
Published: July 12, 2013

activity for hydrogen evolution, which is comparable to that of MoS_2 edge surface sites.[8,9] These trimetallic clusters also efficiently catalyze the evolution of hydrogen when coupled to a p-type Si semiconductor that harvests red photons in the solar spectrum.[10,11] Photocatalytic activity of $NaTiO_3$ for water splitting into H_2 and O_2 has been significantly improved by using Mo_3S_4 molecular complexes as co-catalysts.[12] However, heterogenization of molecular clusters is often limited by leaching phenomena, a problem that can be overcome by tailor-made functionalization of the cluster complex.

The M_3S_4 cluster core is a robust entity, offering unique possibilities of cluster modification from which valuable properties result. Coordination of diphosphine ligands such as in $[M_3S_4Y_3(\text{diphosphine})_3]^+$ (Y = halogen, hydrogen) enhances the cluster stability, and proper functionalization of the ligand with hydroxo group leads to water-soluble clusters that are stable along a wide pH range, in contrast with the $M_3S_4^{4+}$ (aq) species, whose stability is restricted to acidic media.[13] The resulting water-soluble complexes are excellent candidates as catalysts under biphasic conditions or as a co-catalyst to be immobilized in solid surfaces. However, one must take into consideration that small ligand variations can have significant effects on the solubility, reactivity, and aqueous speciation of the resulting molecular clusters. This is the case with $[Mo_3S_4Cl_3(\text{hydroxyalkyldiphosphine})_3]^+$ complexes, for which reactivity, water solubility, and speciation are strongly affected by the length of the alkyl chain. For example, by increasing the length of the hydroxyalkyldiphosphine's alkyl chain from methyl to propyl, water solubility increases by a factor of one hundred.

Speciation studies have identified a complicated set of solution behaviors for these cluster complexes. Although the cluster cation $[Mo_3S_4Cl_3(\text{hydroxyalkyldiphosphine})_3]^+$ maintains its integrity in aqueous HCl solutions for both methyl and propyl ligand chain complexes, the two clusters show remarkable differences under neutral and basic conditions. At neutral pH, the predominant species after dissolving $[Mo_3S_4Cl_3(\text{dhmpe})_3]^+$ (dhmpe = 1,2-bis(bis(hydroxymethyl)-phosphino)ethane) in water has been identified as $[Mo_3S_4(\text{dhmpe})(\text{dhmpe-H})_2(H_2O)]^{2+}$, whereas $[Mo_3S_4Cl_3(\text{dhprpe})_3]^+$ (dhprpe = 1,2-bis(bis(hydroxypropyl)-phosphino)ethane) continues to be the major species in aqueous solution with a minor contribution of the $[Mo_3S_4(\text{dhprpe})(\text{dhprpe-H})_2(H_2O)]^{2+}$ dication. The hydroxyalkyldiphosphine ligand in the dicationic species acts in the tridentate chelating mode, in which ring closure occurs through the substitution of the chlorine atom bonded to the metal by an oxygen atom of the hydroxymethyl chain of the ligand. This clearly exemplifies the noninnocent character of the ligand.[14] Addition of the base to $[Mo_3S_4(\text{dhmpe})(\text{dhmpe-H})_2(H_2O)]^{2+}$ leads to OH^- coordination with the opening of the chelate rings to give the corresponding $[Mo_3S_4(OH)_3(\text{dhmpe})_3]^+$ hydroxo complex. In contrast, the $[Mo_3S_4(\text{dhprpe})(\text{dhmpe-H})_2(H_2O)]^{2+}$ dication closes the chelate ring with the third ligand under basic conditions, with the formation of hydroxo complexes being precluded in this case. Here, we extend our work to other hydroxyalkyldiphosphane complexes, in particular to the dhbupe derivatives (dhbupe = 1,2-bis(bis-(hydroxybuthyl)phosphino)ethane) in order to understand such differences. We have also investigated in parallel the chemistry of the tungsten analogues in order to study the metal's influence in the aqueous speciation of this system.

EXPERIMENTAL SECTION

General Remarks. All reactions were carried out under a nitrogen atmosphere with standard Schlenck techniques. The dhbupe diphosphine and $(Et_4N)_2[Mo_3S_7Cl_6]$ were prepared according to the published methods.[2,15] The starting complexes "$M_3S_4X_4(PPh_3)_3$" were prepared from $(Et_4N)_2[Mo_3S_7Cl_6]$ and PPh_3[16,17] or by excision from polymeric $\{W_3S_7Br_6\}_n$ phases following published procedures.[17] $(H_7O_3)_2[Mo_6Cl_{14}]$ was obtained by dissolving Mo_6Cl_{12} in hot concentrated HCl and allowing the resulting clear yellow solution to cool, giving yellow needles of the product.[18−20] The remaining reactants were obtained from commercial sources and used as received. Solvents for syntheses were dried and degassed by standard methods before use.

Physical Measurements. All manipulations involving free phosphine ligands were carried out under nitrogen. The complexes with phosphines, once formed, are air stable and were handled in air, showing no trace of decomposition. Elemental analyses were performed on an EA 1108 CHNS microanalyzer. $^{31}P\{H\}$ NMR spectra were recorded on a Varian MERCURY 300 MHz or a Varian Inova 400 instrument. Chemical shifts are referenced to external 85% H_3PO_4. Electronic absorption spectra were obtained on a PerkinElmer Lambda-19 or a Cary 50 Bio spectrophotometer. Electrospray ionization mass spectra were recorded with a Q-TOF I (quadrupole-hexapole time-of-flight) mass spectrometer with an orthogonal *Z*-spray electrospray interface (Micromass, Manchester, U.K.) operating at a resolution of approximately 5000 (fwhm). The instrument was calibrated using a solution of NaI in isopropanol/water with m/z ranging from 100 to 1900. Sample solutions (2×10^{-5} M) in water were introduced through a fused-silica capillary to the ESI source via a syringe pump at a flow rate of 10 μL/min. The cone voltage was set to 10 V, unless otherwise stated, to control the extent of fragmentation. Nitrogen was employed as the drying and nebulizing gas. Isotope experimental patterns were compared to the theoretical patterns obtained using the MassLynx 4.0 program.

Kinetic Experiments. The kinetic experiments were carried out with an Applied Photophysics SX-17MV stopped-flow spectrometer provided with a PDA1 photodiode array (PDA) detector. All experiments were carried out at 25.0 °C by mixing an aqueous solution of $[M_3S_4X_3(\text{dhbupe})_3]X$ (M = Mo, W; X = Cl, Br) with a previous treatment (0.05−0.10 M) of HX (X = Cl, Br) or KOH with another solution containing an excess of the other reagents, HX (X = Cl, Br) or KOH. When necessary, the ionic strength was kept constant through the experiments by using the required amounts of KNO_3, KCl, or HNO_3. The solutions of the cluster were prepared at concentrations of $(1.5−5.5) \times 10^{-4}$ M. In all cases, the spectral changes were measured over a wide wavelength range and analyzed with the Specfit program[21] using the kinetic models indicated in the corresponding section.

Synthesis. *$[Mo_3S_4Cl_3(dhbupe)_3]Cl$ ([1]Cl).* $Mo_3S_4Cl_4(PPh_3)_3(H_2O)_2$ (0.100 g, 0.072 mmol) and $(HOCH_2CH_2CH_2\ CH_2)_2PCH_2CH_2P(CH_2CH_2CH_2CH_2OH)_2$ (dhbupe) (0.088 g, 0.230 mmol) were stirred into CH_3CN (25 mL) for 12 h under N_2. A green precipitate, together with some oil, separated. All attempts to filter the product off in air led to it turning completely into a green oil. Therefore, the precipitate was washed only by decantation with CH_3CN (3 × 15 mL) to remove all PPh_3 and then with Et_2O, without filtration, and dried in vacuo. Yield: 0.105 g (85%). NMR $^{31}P\{^1H\}$ (ca. 0.05 M HCl in 1:1 H_2O/D_2O, 121 MHz), δ (ppm): 34.70, 42.20. Anal. Calcd for $C_{54}H_{120}Cl_4Mo_3O_{12}P_6S_4$: C, 38.0; H, 7.1; O, 11.3%. Found: C, 38.3; H, 7.4; O, 12.0%.

$[W_3S_4Br_3(dhbupe)_3]Br$ ([2]Br). $W_3S_4Br_4(PPh_3)_3(H_2O)_2$ (0.100 g, 0.0549 mmol) and $(HOCH_2CH_2CH_2\ CH_2)_2PCH_2CH_2P(CH_2CH_2CH_2CH_2OH)_2$ (dhbupe) (0.066 g, 0.173 mmol) were stirred into CH_3CN (25 mL) for 12 h under N_2. A dark blue precipitate, together with some oil, separated. Attempts to filter the product off in air led to it turning completely into a dark blue oil. The precipitate was washed by decantation with CH_3CN (3 × 15 mL) to remove all PPh_3 and then with Et_2O, without filtration, and dried in vacuo. Yield: 0.094 g (80%). NMR $^{31}P\{^1H\}$ (ca. 0.05 M HCl in 1:1

dx.doi.org/10.1021/ic400897y | Inorg. Chem. 2013, 52, 8713−8722

H_2O/D_2O, 121 MHz), δ (ppm): 11.58, 11.91. Anal. Calcd for $C_{54}H_{120}Br_4W_3O_{12}P_6S_4$: C, 30.2; H, 5.6; O, 8.9%. Found: C, 30.5; H, 5.4; O, 8.8%.

X-ray Studies for $(H_3O)_4[1]_2[Mo_6Cl_{14}]_3$. Single crystals appropriate for diffraction studies were prepared by mixing complex [**1**]Cl (50 mg, 0.031 mmol) dissolved in 1 mL of CH_3OH with 35 mg of $(H_7O_3)_2[Mo_6Cl_{14}]$ (0.029 mmol), also dissolved in 1 mL of CH_3OH, and adding a drop of HCl to the solution. Slow evaporation in an open vial afforded a crop of green crystals suitable for X-ray analysis. Diffraction data were collected at 170 K on an Agilent Supernova diffractometer equipped with an Atlas CCD detector using Mo Kα radiation (λ = 0.710 73 Å). No instrument or crystal instabilities were observed during data collection.[22] Absorption corrections based on the multiscan method were applied.[23,24] The structures were solved by direct methods in SHELXS-97 and refined by the full-matrix method based on F^2 with the program SHELXL-97 using the OLEX software package.[25,26] Crystal data: $C_{54}H_{122}Cl_{24}Mo_{12}O_{14}P_6S_4$, M = 3311.65, triclinic space group $P\bar{1}$, a = 14.5081(4) Å, b = 20.1247(7) Å, c = 25.1681(6) Å, α = 105.456(3)°, β = 103.923(2)°, γ = 105.522(3)°, V = 6427.8(3) Å^3, T = 170 K, Z = 2, μ(Mo Kα) 1.805 mm^{-1}. Reflections collected/unique = 81 900/25 222 (R_{int} = 0.0556). Final refinement converged with R_1 = 0.1043 and R_2 = 0.2375 for all reflections, GOF = 1.058, max/min residual electron density +2.84/−2.28 e/Å^{-3}.

The structure was refined in the triclinic $P\bar{1}$ space group. Anisotropic displacement parameters were refined for all non-H atoms except for the disordered carbon and oxygen atoms of hydroxyalkyl chains. Carbon atom disorder was observed on 3 out of the 12 hydroxybutyl chains, which were refined over two positions. Five oxygen atoms were also refined over two positions. Disordered atoms were all refined with a constraint to the total occupancy of one. The hydrogen atoms bonded to carbon were included at their idealized positions, except for the disordered carbon, and refined as riders with isotropic displacement parameters assigned as 1.2 times the U_{eq} value of the corresponding bonding partner. The hydrogen atoms bonded to oxygen were also treated in a similar way, with isotropic displacement parameters assigned as 1.5 times the U_{eq} value of the corresponding bonding partner. We consider the inclusion of the hydrogen atoms for the disordered CH_2 and OH groups over two positions unjustified. After locating the clusters, two peaks in general positions remained in the difference Fourier map. These peaks were assigned to oxygen from the solvent H_2O molecules and refined anisotropically. The structural figures were drawn using Diamond.[27]

RESULTS AND DISCUSSION

Synthesis, Solid State, and Solution Structures of the 1^+ and 2^+ Complexes and Spectroscopic Studies on Speciation in Aqueous Solution. Polymeric $\{M_3Q_7X_{4/2}X_2\}_n$ one-dimensional phases are the preferred starting material for entry to the chemistry of the incomplete cubane-type M_3Q_4 complexes containing diphosphines, with very few exceptions such as ligand exchange at the preformed Mo_3Q_4 core.[4,28] One such exception is the synthesis of trinuclear molybdenum and tungsten clusters bearing hydroxyakyl phosphine ligands. Recently we have shown that in situ-prepared molecular "$M_3S_4X_4(PPh_3)_3(solv)_2$" species react with hydroxyakyldiphosphines to afford the desired $[Mo_3S_4Cl_3(dihydroxyalkyldiphosphine)_3]^+$ cluster product both for dhmpe (1,2-bis(bis(hydroxymethyl)phosphino)ethane)) and dhprpe, (1,2-bis(bis(hydroxypropyl)phosphino)ethane)).[29,30]

In this work, we have extended the length of the alkyl substituents of the hydroxyakyl phosphine from methyl and propyl to butyl, as represented in eq 1.

$$\text{“}Mo_3S_4Cl_4(PPh_3)_3(solv)_2\text{”} + 3\text{dhbupe} \rightarrow [Mo_3S_4Cl_3(\text{dhbupe})_3]Cl + 3PPh_3 \quad (1)$$

The desired $[Mo_3S_4Cl_3(dhbupe)_3]Cl$, [**1**]Cl, product is isolated in 85% yields. The reaction can be extended to tungsten starting from $W_3S_4Br_4(PPh_3)_3(solv)_2$ to afford $[W_3S_4Br_3(dhbupe)_3]Br$ ([**2**]Br), also in excellent yields. The generality of this synthetic procedure, first applied for the coordination of TTF (tetrathiafulvalene) functionalized diphosphines to Mo_3Q_4 (Q = S, Se), is demonstrated in this work with the isolation of the tungsten cluster analogs.[31]

The molecular structure of $\mathbf{1}^+$ in $(H_3O)_4[\mathbf{1}]_2[Mo_6Cl_{14}]_3$ is shown in Figure 1together with a list of selected bond distances. Bond distances in complex $\mathbf{1}^+$ compare well with those observed for other diphosphino Mo_3S_4 trinuclear clusters.

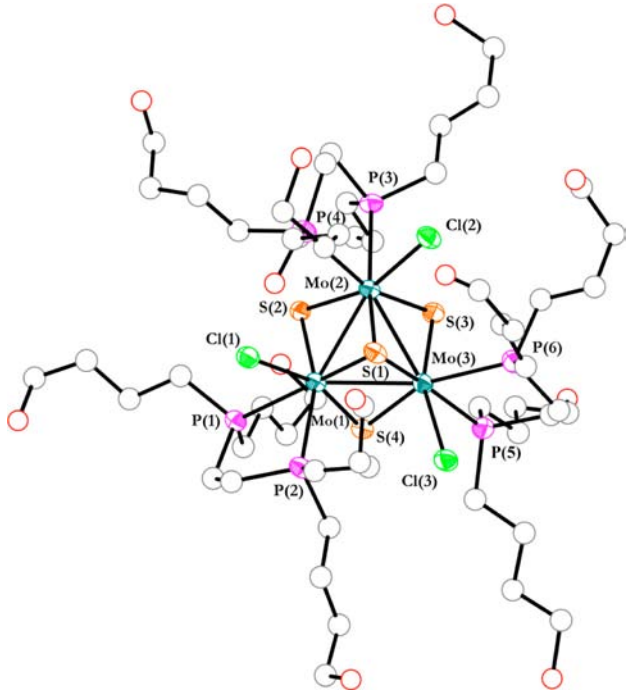

Figure 1. ORTEP representation (50% probability ellipsoids) of the cationic cluster $\mathbf{1}^+$ with the atom numbering scheme. Disordered carbon and oxygen atoms are omitted for clarity. Selected bond lengths (Å): Mo−Mo, 2.7836(11); Mo−(μ_3-(S(1)), 2.363(3); Mo−(μ-(S)-*trans*-P), 2.327(3); Mo−(μ-(S)-*trans*-Cl), 2.278(2); Mo−Cl, 2.494(2); Mo−P(1), 2.546(3); Mo−P(2), 2.608(3).

The $^{31}P\{^1H\}$ NMR spectrum of $\mathbf{1}^+$ in aqueous HCl solution shows two signals at 42.20 and 34.70 ppm (see Figure 2a) in agreement with the solid state structure. All attempts to grow single crystals of $\mathbf{2}^+$ failed; however, like its molybdenum analogue, complex $\mathbf{2}^+$ also presents two signals in its $^{31}P\{^1H\}$ NMR spectrum in aqueous HBr solution at 11.58 and 11.91 ppm (see Supporting Information Figure S1a), which supports a molecular structure for $\mathbf{2}^+$ equivalent to that of $\mathbf{1}^+$. Elemental analysis of [**2**]Br agrees with this formulation. Indirect evidence regarding the formulation of $\mathbf{2}^+$ comes from its speciation studies in aqueous solution, as we will see in the next section.

Water solubility of halogenated molybdenum and tungsten [**1**]Cl and [**2**]Br complexes is moderate (0.005 M) and ranges between that of its dihydroxyproyl analog (0.1 M) and the limited water solubility of the dihydroxymethyl complex (0.001 M). A decrease in water solubility upon increasing the length of the ligand alkyl chain is expected; however, there must be other reasons behind the low solubility of the $[Mo_3S_4Cl_3(dhmpe)_3]Cl$ salt that we attribute to the formation of oligomers upon

dx.doi.org/10.1021/ic400897y | Inorg. Chem. 2013, 52, 8713−8722

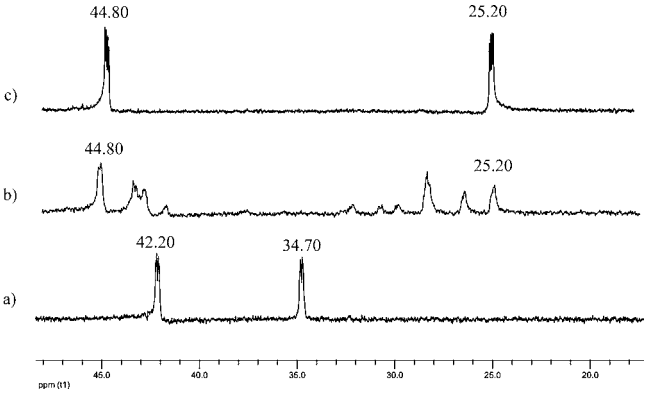

Figure 2. $^{31}P\{^{1}H\}$ NMR spectra of $\mathbf{1}^{+}$ in (a) 0.05 M HCl (aq) and (b) H_2O and of $\mathbf{1}_{OH}^{+}$ in (c) 0.05 M NaOH (aq).

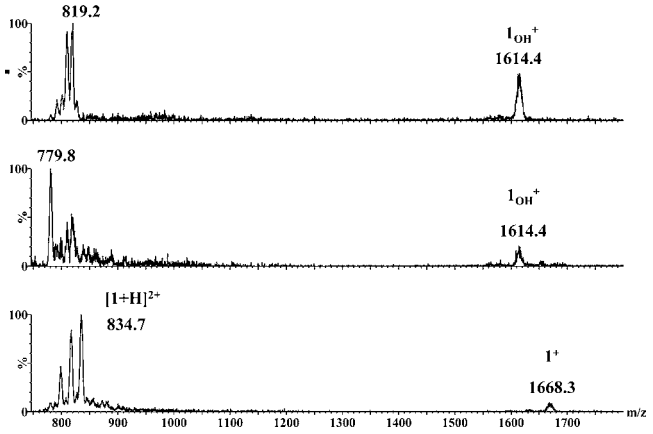

Figure 3. ESI-MS spectra of 2×10^{-5} M solutions of compound **1**[Cl] at U_c = 10 V in H_2O (middle) and in the presence of aqueous 0.001 M HCl (bottom) and 0.001 NaOH (top). In these experiments, the added amount of HCl or NaOH was limited due to the ionization inhibition effects.

displacement of the Cl atom of a cluster unit by the hydroxo group of the diphosphine of a neighbor cluster. As pointed out in the Introduction, the ligand hydroxo groups play a noninnocent role, and this fact conditions the behavior of these complexes in aqueous solutions and the kinetics of their substitution reactions, as we will detail in the next section.

As previously observed for clusters with the related dhmpe and dhprpe ligands,[29,30] the $^{31}P\{^{1}H\}$ NMR spectra of [**1**]Cl or [**2**]Br in aqueous solution (Figures 2b and Supporting Information S1b) are relatively crowded due to the partial substitution of one (or two) of the Cl ligands, which causes a lowering of symmetry from C_3 to C_1; consequently, up to six phosphorus resonances are observed for each species.[32−35] Because the spectra show more than six signals, it is evident that the solutions contain a mixture of species. In contrast, solutions containing added HCl or HBr lead to spectra with only two phosphorus signals (Figures 2a and Supporting Information S1a), as expected for C_3 symmetry clusters with three equivalent diphosphines, in agreement with the $\mathbf{1}^{+}$ structure. Noticeably, $^{31}P\{^{1}H\}$ NMR spectra are significantly affected by the cluster concentration, which suggest the occurrence in solution of equilibria involving chloride dissociation in a way similar to that previously reported for the related dhprpe clusters.[30] Addition of NaOH to aqueous solutions of [**1**]Cl or [**2**]Br restores the C_3 symmetry of the cluster, and only two phosphorus signals are observed for both molybdenum and tungsten. The chemical shifts differ from those of the starting complexes, so new species are being generated (Figures 2c and Supporting Information S1c). Unfortunately, all attempts to isolate the products that formed in basic solution as solids failed due to formation of oils, so the characterization of these species was completed by ESI-MS techniques, which have also proved to be very useful for the characterization and reactivity studies of related M_3Q_4 complexes.[29,30,36]

The ESI mass spectrum of aqueous 2×10^{-5} M solutions of [**1**]Cl in Figure (middle) shows a prominent peak centered at m/z = 779.8 that can be attributed to the chlorine-free $[Mo_3S_4(dhbupe)(dhbupe\text{-}H)_2]^{2+}$ dication on the basis of the m/z value and its characteristic isotopic pattern.[29,30] Because such formulation implies a vacant site in one of the metals, we cannot rule out that the signal at m/z = 779.8 results from dissociation of the coordinated water molecule from $[Mo_3S_4(dhbupe)(dhbupe\text{-}H)_2(H_2O)]^{2+}$. Precedents for this formulation come from our earlier investigations on the homologous dhmpe and dhprpe cluster complexes.[29,30] Upon acidification of aqueous solutions of [**1**]Cl with HCl, the signal expected for intact $\mathbf{1}^{+}$ at m/z = 1668.3 is observed together with a doubly charged peak at m/z = 834.7 associated to the protonated species $[\mathbf{1}+H]^{2+}$ (Figure 3, bottom). Two extra peaks due to chlorine decoordination, $[\mathbf{1}-Cl]^{2+}$ at m/z = 817.4 and $[Mo_3S_4Cl(dhbupe)_2(dhbupe\text{-}H)]^{2+}$ at m/z = 797.7, are also seen in the same region. For the tungsten cluster complex, a peak due to the $[W_3S_4(dhbupe)(dhbupe\text{-}H)_2]^{2+}$ dication (m/z = 912.4) is also seen as the most intense signal at neutral pH; however, in this case, addition of HBr to an aqueous solutions of [**2**]Br does not significantly change the appearance of the spectrum, and the signal at m/z = 912.4 remains as the only peak (see Supporting Information Figure S2).

The apparent discrepancies regarding the predominant species in solution that are inferred from $^{31}P\{^{1}H\}$ NMR and ESI-MS techniques can be attributed to differences in sample concentration that strongly affect the ratio of the different species in solution. Thus, where both techniques agree that aqueous solutions of [**1**]Cl and [**2**]Br essentially contain halogen-free dications of formula $[Mo_3S_4(dhbupe)(dhbupe\text{-}H)_2(H_2O)]^{2+}$ or $[W_3S_4(dhbupe)(dhbupe\text{-}H)_2]^{2+}$, signals corresponding to intact $\mathbf{1}^{+}$ and $\mathbf{2}^{+}$ cations as the major product in acidic HCl or HBr solutions are only observed by $^{31}P\{^{1}H\}$ NMR spectroscopy. For the molybdenum system, ESI mass spectra on acidic HCl solutions show other peaks in addition to the ones that are due to the expected intact $\mathbf{1}^{+}$ cation and which result from the partial dissociation of the halide ligands. Unexpectedly, the ESI spectra of aqueous solutions of $\mathbf{2}^{+}$ do not significantly change upon the addition of HBr, in apparent contradiction with the $^{31}P\{^{1}H\}$ NMR results. Despite the inherent differences between the spectroscopic and spectrometric techniques related to the concentration intervals accessible for each technique that differ by at least 3 orders of magnitude, both techniques evidence that the speciation in [**1**]Cl and [**2**]Br solutions is dominated by halogen-free species as the solutions are diluted in water.

When NaOH solutions of [**1**]Cl were investigated by ESI-MS (Figure 3, top), doubly and singly charged peaks at m/z = 819.2 and 1614.4 are observed due to the appearance of $[Mo_3S_4(OH)_3(dhbupe)_3+Na]^{2+}$ and $[Mo_3S_4(OH)_3(dhbupe)_3]^{+}$ ($\mathbf{1}_{OH}^{+}$) cations, respectively. This formulation is in agreement with the two signals observed in the $^{31}P\{^{1}H\}$

dx.doi.org/10.1021/ic400897y | Inorg. Chem. 2013, 52, 8713−8722

NMR spectra and the recovery of the C_3 symmetry upon addition of a base to aqueous solutions of the $\mathbf{1}^+$ cation. This fact unequivocally evidences the solution structure of a new hydroxo trinuclear cluster formed in basic media. Similar results are obtained for the $\mathbf{2}^+$ tungsten compound, where one peak due to $[W_3S_4(OH)_3(dhbupe)_3]^+$ ($\mathbf{2}_{OH}^+$) at m/z = 1877.4 is observed together with a doubly charged peak that results from the doubly charged sodium-containing adduct. The formation of trishydroxo complexes found for the dhbupe clusters under basic conditions was previously observed for $[Mo_3S_4Cl_3(dhmpe)_3]^+$, and it contrasts with the behavior found for the $[Mo_3S_4Cl_3(dhprpe)_3]^+$ cluster complex where addition of a base causes the closure of three six-member M−O−C−C−C−P rings to afford the $[M_3S_4(dhmpe\text{-}H)_3]^+$ cation.[29,30] For the hydroxybutyl system, coordination of the oxygen from the ligand's hydroxo group does not take place, probably because the formation of seven-member ring structures is not favored and tris hydroxo complexes are obtained instead. Tyler et al. have found a similar situation when investigating monometallic iron complexes, but in their case, coordination of the noninnocent hydroxyl diphoshpine group does not involve its deprotonation.[14]

The UV−vis spectra of solutions containing [**1**]Cl and [**2**]Br were recorded under different conditions to obtain the spectra of the different species formed. The spectra of $\mathbf{1}^+$ and $\mathbf{1}_{OH}^+$, represented in Figure 4a, were obtained by using 0.025 M HCl

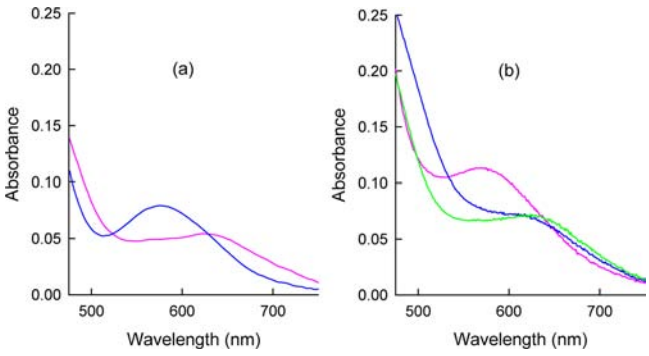

Figure 4. UV−vis spectra at 25 °C for aqueous solutions of [**1**]Cl and [$\mathbf{1}_{OH}$]Cl under different conditions. (a) [**1**]Cl in 0.025 M HCl (pink line, λ_{max} = 627 nm) and [$\mathbf{1}_{OH}$]Cl in 0.025 M KOH (blue line, λ_{max} = 575 nm); cluster concentration = 1.5×10^{-4} M. (b) [**1**]Cl in 0.15 M Hpts (blue line, shoulder at ca. 600 nm), [**1**]Cl in 0.15 M NaCl (green line, λ_{max} = 627 nm), and [**1**]Cl in 0.15 M KOH (pink line, λ_{max} = 575 nm); cluster concentration = 2.7×10^{-4} M.

and 0.025 M KOH, respectively, and they each show one band at 627 and 575 nm, respectively. To be able to discriminate between possible separate effects of H^+ and Cl^-, additional experiments were carried out using Hpts (pts = *p*-toluenesulfonate) instead of HCl. In 0.03−0.15 M Hpts (see Figure 4b), the spectrum is clearly different from those in Figure 4a and shows a shoulder at ca. 600 nm, but it evolves to show the bands for the chloro and hydroxo species when an excess of NaCl or KOH is added. Similar spectra were obtained in additional experiments using HNO_3 instead of Hpts, which indicates that there are no coordinated nitrate or para-toluenesulfonate anions under those conditions, so that the shoulder at 600 nm must be associated with the presence of protons. Similar results were obtained for the tungsten complexes, which show bands at 556 nm for $\mathbf{2}^+$ and at 510 nm for $\mathbf{2}_{OH}^+$ (see Supporting Information Figure S3), while the spectrum in Hpts solution shows a shoulder at ca. 525 nm. It was also observed during the experiments that [**2**]Br decomposes in aged acidic solutions, so that the maximum of absorbance is shifted in 24 h from 555 to 570 nm (Supporting Information Figure S3) when $[H^+]_f$ = 0.025 M.

With regard to the nature of the species formed in acidic solutions in the absence of coordinating anions, two possibilities based on previous results with clusters of related ligands exist: formation of aqua complexes or formation of species with a chelate ring formed with a deprotonated hydroxyl group in the substituted diphosphine. However, the latter possibility can be reasonably ruled out because formation of those species requires deprotonation and occurs in basic solutions,[30] whereas in the present case, the new species are formed upon addition of an acid excess. Thus, the most reasonable explanation is that when an excess of acid with a noncoordinating anion is added to a solution containing the hydroxo cluster, the OH^- ligands become protonated and an aqua cluster is formed. In an attempt to determine if the process occurs at all three of the metal centers or only at some of them, $^{31}P\{^1H\}$ NMR spectra of solutions with added Hpts were recorded. Those spectra show multiple signals and resemble those in Figure 2b, thus showing that a mixture of species exist in solution (i.e., complete conversion to the triaqua species is not achieved). This finding is not surprising when the acidity of coordinated water in M_3S_4 clusters is considered, as some of the coordinated water molecules in $M_3S_4(H_2O)_9^{4+}$ clusters (M = Mo, W) have been shown to deprotonate even in strongly acidic solutions.[37,38]

Kinetic Studies Related to the Aqueous Speciation of [1]Cl and [2]Br. To avoid the complications caused by the mixtures of species in aqueous solutions of [**1**]Cl and [**2**]Br, kinetic studies were carried out with solutions containing added HX (X = Cl or Br) or KOH at a concentration large enough (0.025 or 0.050 M) to ensure complete conversion to the trihalide or trihydroxide forms, respectively. In this way, it is expected that the kinetics of the reaction in Scheme 1 could be studied in both directions by adding an excess of the other reagent; that is, base addition to the trichloro or tribromo complexes will cause halide substitution by OH^-, whereas addition of HX to the trihydroxo complexes will lead to the trihalo complexes. The situation is quite similar to that previously found for the related dhprpe cluster[30] except that no hydroxo complexes were formed in that case, and basic solutions contained chelated species with an alkoxo group coordinated at each metal center. Thus, the present dhbupe clusters provide an excellent opportunity to complete the kinetic study of the reactions relevant to speciation of this kind of cluster in an aqueous solution, and a comparison between the kinetics associated with the OH^- coordination/dissociation (dhbupe clusters) can be made with those of the chelate ring closure/opening (dhprpe clusters).

Kinetics of the Substitution of Halide Ligands by Hydroxo Groups. The reactions of [**1**]Cl and [**2**]Br with an excess of base have been studied using KOH (0.05−0.475 M) at two concentrations of acid ([HX] = 0.025 and 0.050 M, X = Cl and Br). In all cases, the reaction occurs in the time scale of the stopped-flow technique. Although very small spectral changes are also observed at longer times, they do not lead to any change in the position of the absorption maxima and can be attributed to secondary processes (i.e., precipitation).

The spectral changes in the reaction of [**1**]Cl with a base to produce $[Mo_3S_4(OH)_3(dhbupe)_3]^+$ ($\mathbf{1}_{OH}^+$) are illustrated in

dx.doi.org/10.1021/ic400897y | *Inorg. Chem.* 2013, 52, 8713−8722

Scheme 1Substitution Reactions of Halide Ligands by Hydroxo Groups in 1^+ and 2^+ To Afford $\mathbf{1}_{OH}^+$ and $\mathbf{2}_{OH}^+$, and Vice Versa.

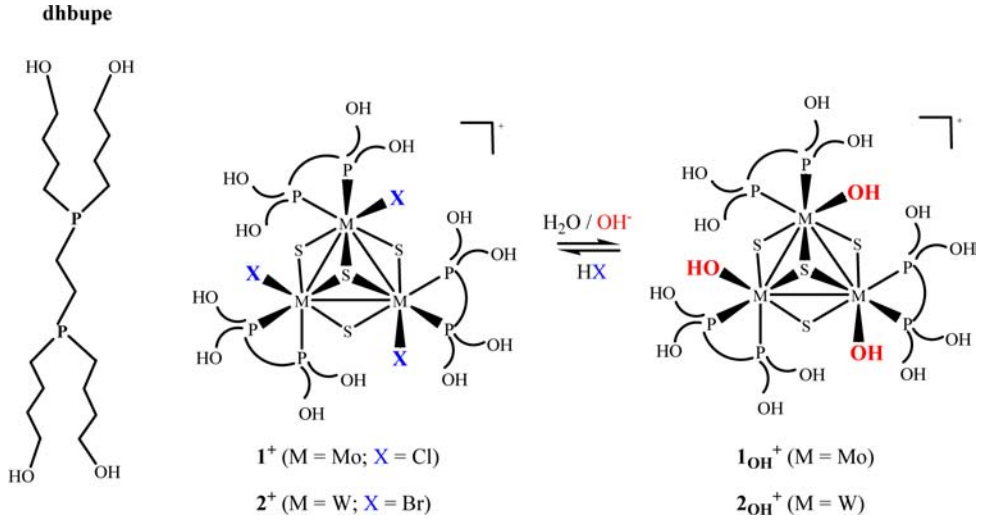

Figure 5. The reaction is completed in 1−2 s, and the changes can be satisfactorily fitted to a kinetic model with a single exponential. The calculated spectra (Figure 6) show a shift of the maximum from 627 to 575 nm, which coincides with the values expected for substitution of the three chlorides by hydroxide ligands (see previous section). Because a single kinetic step is resolved for the three consecutive substitutions, the conclusion is that the reaction proceeds at the three metal centers with statistically controlled kinetics, and the numerical values of k_{obs} correspond to the rate constant for reaction at the third metal center.[39−43] The values of k_{obs} show a linear dependence with the base concentration; as shown in Figure 7, similar results are obtained regardless of the HCl concentration, so all data were fitted together using eq 2 to afford a value of $b = 22 \pm 3\ M^{-1}\ s^{-1}$.

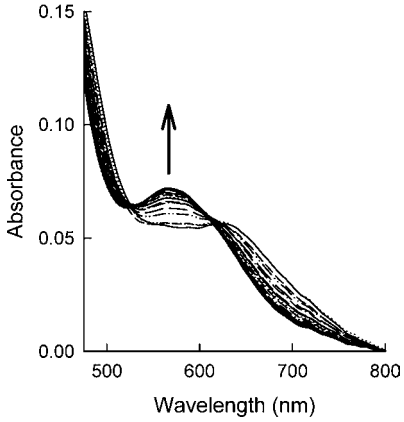

Figure 5. Typical spectral changes for the reaction of [**1**]Cl with base, which yields [$\mathbf{1}_{OH}$]Cl (T = 25.0 °C, cluster concentration = 1.5×10^{-4} M, reaction carried out with a starting solution containing 0.025 M HCl).

$$k_{obs} = b[OH^-] \quad (2)$$

In contrast, the spectral changes observed for the reaction of [**2**]Br with base to form [$\mathbf{2}_{OH}$]Br (see Supporting Information Figure S4) require a kinetic model with three consecutive exponentials. This analysis provides calculated spectra for all species formed at the different stages of the reaction, and they are included in Supporting Information Figure S5. In some

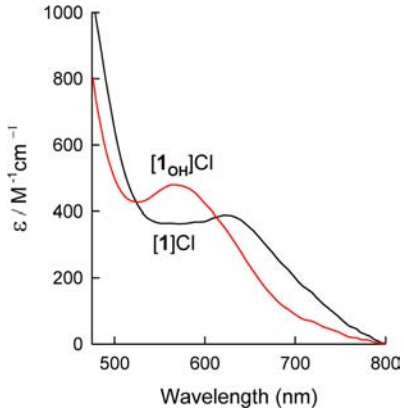

Figure 6. Electronic spectra calculated for the starting complex and the reaction product by fitting the spectral changes in Figure 5 to a single exponential.

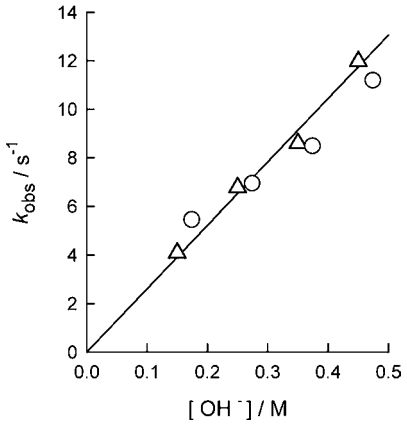

Figure 7. Plot showing the [OH^-] dependence of the observed rate constant for the reaction of [**1**]Cl with base to form [$\mathbf{1}_{OH}$]Cl. The data correspond to two sets of experiments with starting solutions containing different concentrations of HCl (0.025 and 0.05 M as circles and triangles, respectively).

dx.doi.org/10.1021/ic400897y | Inorg. Chem. 2013, 52, 8713−8722

cases, additional spectral changes are also observed at longer times, but they are again very small and irreproducible, so they can be reasonably attributed to secondary processes.

The overall spectral changes show a shift of the absorbance band from approximately 555 to 509 nm, in agreement with the conversion of the tribromide to the trihydroxide cluster, and the calculated spectra in Supporting Information Figure S5 show that this conversion occurs with the formation of reaction intermediates with maxima at 542 and 516 nm, their molar absorptivity values also being intermediate between those of the starting and final products. However, although these spectra show gradual changes that suggest that the metal centers behave as independent chromophores, simplification to a single exponential is not observed because the rate constants for the three consecutive steps deviate with respect to those corresponding to the 3:2:1 ratio expected from statistics, which contrasts with the statistically controlled kinetics observed for the molybdenum system.

There is an additional important difference between the molybdenum and tungsten clusters in the order of reaction with respect to OH^-; whereas the order is one for the single step resolved for [**1**]Cl, the values of k_{obs} for the three stages in the reaction of [**2**]Br are independent of the base concentration and do not change significantly with the bromide concentration; the mean values for experiments at two different Br^- concentrations are $k_1 = 27 \pm 8\ s^{-1}$, $k_2 = 0.7 \pm 0.1\ s^{-1}$, and $k_3 = 0.13 \pm 0.02\ s^{-1}$. Moreover, the independence of the rate constants in the presence of an excess of the leaving ligand observed for substitutions in the two clusters rules out a dissociative mechanism for the formation of the trihydroxo clusters.

Kinetics of Substitution of OH^- Groups by Halide Ligands. No spectral changes were observed after mixing the [$\mathbf{1}_{OH}$]Cl and [$\mathbf{2}_{OH}$]Br tris(hydroxide) clusters with potassium or *n*-tetrabutylammonium chloride or bromide salts. However, the conversion of [$\mathbf{1}_{OH}$]Cl and [$\mathbf{2}_{OH}$]Br into[**1**]Cl and [**2**]Br is easily achieved using an excess of HCl or HBr; therefore, protons must be present for the substitution reaction to take place.

In the case of [$\mathbf{1}_{OH}$]Cl, the spectral changes (see Supporting Information Figure S6) can be fitted with a single exponential (model A → B), which yields the calculated spectra in Supporting Information Figure S7. As the maximum calculated for A (ca. 600 nm) does not match that for [$\mathbf{1}_{OH}$]Cl (575 nm), those experiments indicate that there are additional spectral changes that occur within the stopped-flow mixing time. However, the spectrum of A agrees well with that obtained upon addition of Hpts or HNO_3 (Figure 4b), so it can be concluded that upon addition of an acid excess the OH^- ligands are protonated to generate aqua clusters that evolve to the reaction product. As the maximum calculated for B (627 nm) agrees well with the spectrum of [**1**]Cl, the spectral changes observed correspond to coordination of three chlorides. The existence of a single resolved step suggests that the process occurs with statistically controlled kinetics. The values of k_{obs} show a first-order dependence with the acid concentration (Figure 8), and fitting the data to eq 3 gives $c = 8 \pm 2\ s^{-1}$ and $d = 95 \pm 6\ M^{-1}\ s^{-1}$.

$$k_{obs} = c + d[HX]_0 \quad (3)$$

The spectral changes for the reaction of [$\mathbf{2}_{OH}$]Br with HBr (Supporting Information Figure S8) are even more complex, and a satisfactory fit requires a model with three consecutive steps (A → B→ C → D; see calculated spectra in Supporting Information Figure S9). Again, the spectrum calculated for A (525 nm) indicates protonation of the coordinated hydroxo groups within the stopped-flow mixing time. Comparison of the spectrum for [**2**]Br to those calculated for B, C, and D indicates that conversion to the tribromo cluster occurs in the first resolved kinetic step. The dependence of the rate constant for this step on the HBr concentration is also illustrated in Figure 8 and can also be fitted with eq 3 to give $c = 4 \pm 1\ s^{-1}$ and $d = 43 \pm 3\ M^{-1}\ s^{-1}$. On the other hand, species C and D show an absorption band at ca. 570 nm, which suggests that they are secondary products formed in the presence of an excess of acid. This interpretation agrees with NMR and UV−vis observations that show some instability of the cluster in solution, especially at longer times. Actually, NMR spectra of aged solutions show the appearance of signals for mononuclear species, and the UV−vis spectrum shows that the absorption maximum is shifted to 568−570 nm.

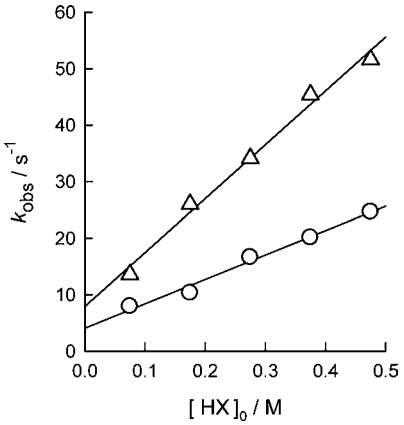

Figure 8. Plots showing the $[HX]_0$ dependence of the observed rate constant for the reaction of [$\mathbf{1}_{OH}$]Cl or [$\mathbf{2}_{OH}$]Br with acid to form [**1**]Cl (triangles) or [**2**]Br (circles).

Additional experiments were carried out to separate the effects of the protons and halide anions on the kinetics of reaction. In those experiments, the concentration of one ion was kept constant and the other one was changed. Two series of experiments were carried out for each cluster by keeping the proton concentration constant at two different values (0.475 and 0.075 M), whereas the chloride or bromide concentration was changed within each series. Unfortunately, for both clusters, the experiments with $[H^+] = 0.075$ M show very small spectral changes that lead to rate constants with large errors and poor reproducibility, so only the experiments with $[H^+] = 0.475$ M could be analyzed. In this case, the observations were similar to those for the reaction with HX, with spectral changes that occur within the stopped-flow mixing time and k_{obs} values that show a linear dependence with the anion concentration (see Figure S10 in Supporting Information and compare with Figure 8). Actually, fitting the data with eq 4 leads to *c* and *d* values similar to those obtained in the experiments with HCl or HBr: $c = 4 \pm 3\ s^{-1}$ and $d = 94 \pm 10\ M^{-1}\ s^{-1}$ for [$\mathbf{1}_{OH}$]Cl, and $c = 5 \pm 1\ s^{-1}$ and $d = 40 \pm 3\ M^{-1}\ s^{-1}$ for [$\mathbf{2}_{OH}$]Br. The larger discrepancies found between the *c* values derived for the Mo cluster are probably related to the larger errors associated with the data at the lower concentrations of acid in Figure 8. Because the values of *c* and *d* are independent of the proton concentration, it can be concluded that there is no acid-dependent term in the rate law,

dx.doi.org/10.1021/ic400897y | *Inorg. Chem.* 2013, 52, 8713−8722

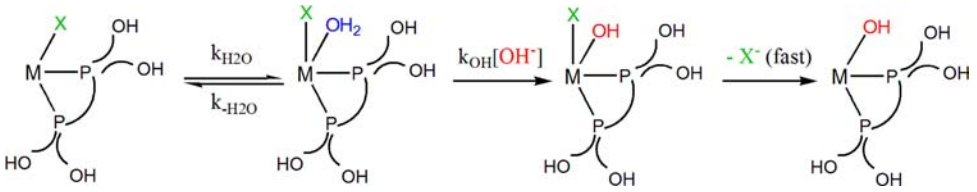

Figure 9. Reaction mechanism for the substitution of coordinated halide by OH^-, leading to the rate law in eq 7. Simplification to an OH^--independent rate law requires consideration of the water attack as the rate-determining step, whereas simplification to first-order with respect to OH^- requires that the rate-determining step is displaced by the OH^- attack.

so the concentration dependence of the rate constant is represented by eq 4. The whole of this information thus indicates that the conversion of $\mathbf{1}_{OH}^+$ or $\mathbf{2}_{OH}^+$ to $\mathbf{1}^+$ or $\mathbf{2}^+$ occurs with OH^- protonation within the stopped-flow mixing time followed by substitution of water by X^- (eq 5).

$$k_{obs} = c + d[X^-] \tag{4}$$

$$\mathbf{1}_{OH}^+ \text{ or } \mathbf{2}_{OH}^+ \xrightarrow{H^+,\ fast} \mathbf{1}_{OH_2}^+ \text{ or } \mathbf{2}_{OH_2}^+ \xrightarrow{X^-,\ k_{obs}} \mathbf{1}^+ \text{ or } \mathbf{2}^+ \tag{5}$$

Mechanistic Considerations. The different rate laws observed for the reactions of the Mo and W clusters provide very useful mechanistic information that adds to that previously reported for related systems.[29,30] One main consideration concerns relative rates of reaction at the three metal centers. Classical studies by the group of Sykes showed that substitutions in the $[M_3Q_4(H_2O)_9]^{4+}$ clusters occur in aqueous solution with statistical kinetics,[39,41] which indicates that the expected three-phase kinetics is simplified to a single phase because the metal centers behave as independent chromophores, and the rate constants for reaction at the three centers are in the statistical 3:2:1 ratio. Some recent re-examinations using diode-array detection and global analysis of the kinetic data essentially confirm those conclusions.[44] The mathematical requirements for simplification to a single exponential have also been discussed on the basis of DFT and TD-DFT calculations, and it has been shown that simplification to a single exponential is still possible even in cases where the ratio of the successive rate constants differ from the statistical prediction.[43] Actually, reaction at a metal center is reasonably expected to affect the kinetics of reaction at the other centers, so deviation of the rate constants from the statistical prediction should be expected to be observed more frequently. However, previous kinetic studies on reactions of $[M_3S_4X_3(\text{diphosphine})_3]^+$ clusters, where the diphosphine contains hydroxyalkyl groups, have provided examples of both statistical kinetics and deviations from it.[29,30] A similar situation arises in the present work, so that these systems are in the borderline for the simplification of the rate law to a single exponential. Although the reasons for the existence or the lack of those deviations are not clear yet, the analysis of the numerical values of the rate constants and the spectra calculated for the reaction intermediates indicates that, at least in the present cases, the three metal centers can be reasonably considered to behave as independent chromophores (Supporting Information Figure S5), and deviations arise because the ratio of the rate constants deviates significantly with respect to the 3:2:1 statistical ratio, with values of 100:10:1 for the Mo cluster with dhmpe,[29] or the 208:5:1 ratio in the present work for the W cluster with dhbupe.

Another important aspect of the kinetic results in the present work is that rate laws usually have two terms, one dependent on and the other independent of the entering ligand. Thus, the kinetics of reaction of the aqua clusters with X^- obeys the rate law in eq 4, where c and d correspond to the halide-independent and -dependent terms, respectively. The relative contribution of both pathways depends on the concentration of the entering ligand, although in general the contribution of the c pathway is smaller. For the reaction in the reverse direction, the situation is not so evident because the W cluster shows kinetics independent of the OH^- concentration, whereas the Mo analogue only shows a term with a first-order dependence with respect to OH^-. However, both rate laws can be considered to arise from different simplifications of the common 2−term rate law in eq 6. In that case, the a and b terms would correspond to attacks by water or OH^- anions, respectively, and each one of the clusters would react exclusively through one of those pathways. Although there is an alternative common rate law that would also allow both simplifications (eq 7, Figure 9), we think that eq 6 is favored because simplification of eq 7 to a to first-order process with respect to OH^- requires considering that the rate-determining step is displaced by the OH^- attack, which is unlikely because it is a presumably fast proton transfer process, and so it could not be rate-limiting.

$$k_{obs} = a + b[OH^-] \tag{6}$$

$$k_{obs} = \frac{k_{OH}k_{H_2O}[OH^-]}{k_{-H_2O} + k_{OH}[OH^-]} \tag{7}$$

Two-term rate laws, such as those in eqs 4 and 6, can arise from the existence of two parallel reaction pathways or from a contribution by the rate of the reverse reaction in a reversible process. However, the latter possibility can be reasonably excluded in the present case because the absorbance changes are similar for different concentrations of the entering ligand even in the case of the reaction between [**2**]Br and OH^-, where the spectral changes show complete formation of the trihydroxo complex despite the rate law only showing an OH^--independent term. Thus, the reaction in Scheme 1 appears to occur through two parallel pathways in both directions, but in the case of the reaction with HX, the process actually occurs at the aqua cluster formed upon protonation of coordinated hydroxo groups. Direct substitution of OH^- by X^- is not observed when salts are used in the absence of acid. One of the pathways involves a rate-determining direct attack of the entering ligand, X^- or OH^- depending on the direction (b and d pathways in Figure 10). The process could go through formation of an outer-sphere complex or with formation of an intermediate containing both coordinated OH^- and X^- in a pseudoassociative pathway similar to that recently proposed for substitutions in related clusters, which according to DFT calculations is made possible because the cluster core is able to undergo a structural reorganization that allows for accom-

dx.doi.org/10.1021/ic400897y | Inorg. Chem. 2013, 52, 8713−8722

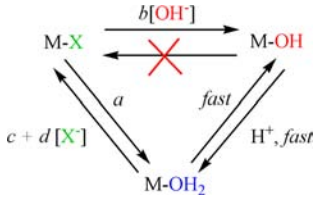

Figure 10. Reaction mechanism proposed for the interconversion between $\mathbf{1}_{OH}^{+}$ or $\mathbf{2}_{OH}^{+}$ and $\mathbf{1}^{+}$ or $\mathbf{2}^{+}$. The upper pathway involves direct reaction and the lower pathway goes through an intermediate containing coordinated water.

modation of the excess of electron density.[42,45] As we pointed out above, the *c* term also corresponds to a minor pathway in the formation of the halogen-containing clusters, and there is even the possibility that its appearance is simply a consequence of larger errors in the kinetic data at the lower concentrations of acid. In any case, the precise mechanistic details of this pathway cannot be established. The *a* pathway corresponds to the formation of the hydroxo cluster through water attack followed by deprotonation. The reasons leading to the operation of one pathway or the other are not clear with the information currently available, but the larger size of bromide would hinder an associative attack such as is probably occurring in the *d* pathway.

CONCLUSIONS

The present studies on water-soluble molybdenum and tungsten clusters with the dhbupe diphosphine complement those previously reported for related diphosphines with shorter hydroxyalkyl substituents, so enough information is gathered regarding the synthesis and structure as well as their speciation and substitution reaction kinetics on $[M_3S_4(X,OH)_3(dihydroxyalkyldiphosphine)_3]^+$ clusters. Molybdenum and tungsten $[M_3S_4X_3(dhbupe)_3]^+$ (M = Mo and X = Cl or M = W and X = Br) complexes are prepared in good yields, and they possess a cuboidal M_3S_4 structure, with the outer positions occupied by the two phosphorus atoms and a halide ligand. The behavior of these clusters in neutral aqueous solution is very complex, with formation of a variety of species that make meaningless the NMR spectra of aqueous solutions of these clusters. NMR and ESI-MS techniques evidence that aqueous solutions of $[M_3S_4X_3(dhbupe)_3]^+$ are dominated by halogen-free species. Apparent discrepancies regarding the predominant species in solution using both techniques can be attributed to differences in the concentration interval, as previously found for their dhprpe analogues.

Remarkably, the nature of the species formed in a basic solution is very different for the dhprpe and dhbupe ligands. Whereas dhprpe forms chelated species, dhbupe forms hydroxo complexes, surely as a consequence of the different stability achieved with six- and seven-member chelate rings. The values of the rate constants measured for the different diphosphines are within the 0.01−50 s^{-1} range for all the reactions studied to date with the three hydroxyalkyl-substituted diphosphines containing alkyl chains of different lengths, and the rate laws usually reveal the existence of parallel reaction pathways. One of the pathways is usually first order with respect to the entering ligand and can be accommodated with a pseudoassociative mechanism in which both the entering and leaving ligands coordinate simultaneously to the metal center, probably with structural reorganization of the cluster core to allow for the excess electron density. The other pathway is zero order with respect to OH^- or the corresponding entering ligand, and it surely goes through the formation of aqua clusters or species with chelate rings. Chelated species can be stabilized by using the hydroxypropyl substituent that leads to the optimal size of the chelate ring, but they are formed quantitatively only in basic solution. When the size of the hydroxyalkyl chains increase, formation of the chelate ring is not favored, and basic solutions contain hydroxo clusters. At this point, it is interesting to consider what would happen for clusters with the related 1,1-bis(bis(hydroxyethyl)phosphine)ethane) ligand, which would lead to 5-member chelate rings. The stability of those rings make it reasonable to expect formation of chelated species, but the complex behavior found for clusters with this kind of substituted diphosphines makes anticipating the results risky.

ASSOCIATED CONTENT

Supporting Information

CIF and listings of spectroscopic, spectrometric, and kinetic data for the $\mathbf{2}^{+}$ and $\mathbf{2}_{OH}^{+}$ complexes. This material is available free of charge via the Internet at http://pubs.acs.org.

AUTHOR INFORMATION

Corresponding Author

*R.L.: e-mail, rosa.llusar@uji.es; fax, +34 964 728066; phone, +34 964 728086. M.G.B: e-mail, manuel.basallote@uca.es; fax, +34 956 016288; phone, +34 956 016339.

Notes

The authors declare no competing financial interest.

ACKNOWLEDGMENTS

The financial support of the Spanish Ministerio de Economia y Competitividad (Grants CTQ2012-37821-C02-02, CTQ2011-23157, and CTQ2009-14443-C02-01), Fundació Bancaixa-UJI (research project P1.1B2010-46) and Generalitat Valenciana (ACOMP/2011/037 and Prometeo/2009/053), and Junta de Andalucía (Grupo FQM-137, Grant P07-FQM-02734) is gratefully acknowledged. The authors also thank the Servei Central D'Instrumentació Cientifica (SCIC) of the Universitat Jaume I and the Servicios Centrales de Ciencia y Tecnología of the Universidad de Cádiz for providing us with the mass spectrometry, NMR, and X-ray facilities. T.B. thanks the Spanish Ministerio de Ciencia e Innovación (MICINN) for a doctoral fellowship (FPI). J.A.P.C. also acknowledges Junta de Andalucía for a doctoral fellowship.

REFERENCES

(1) Shaughnessy, K. H. *Chem. Rev.* **2009**, *109*, 643.
(2) Baxley, G. T.; Weakley, T. J. R.; Miller, W. K.; Lyon, D. K.; Tyler, D. R. *J. Mol. Catal. A: Chem.* **1997**, *116*, 191.
(3) Holz, J.; Heller, D.; Sturmer, R.; Borner, A. *Tetrahedron Lett.* **1999**, *40*, 7059.
(4) Llusar, R.; Uriel, S. *Eur. J. Inorg. Chem.* **2003**, 1271.
(5) Seino, H.; Hidai, M. *Chem. Sci.* **2011**, *2*, 847.
(6) Beltran, T. F.; Feliz, M.; Llusar, R.; Mata, J. A.; Safont, V. S. *Organometallics* **2011**, *30*, 290.
(7) Sorribes, I.; Wienhoefer, G.; Vicent, C.; Junge, K.; Llusar, R.; Beller, M. *Angew. Chem., Int. Ed.* **2012**, *51*, 7794.
(8) Jaramillo, T. F.; Bonde, J.; Zhang, J.; Ooi, B.-L.; Andersson, K.; Ulstrup, J.; Chorkendorff, I. *J. Phys. Chem. C* **2008**, *112*, 17492.
(9) Merki, D.; Hu, X. *Energy Environ. Sci.* **2011**, *4*, 3878.
(10) Hou, Y.; Abrams, B. L.; Vesborg, P. C. K.; Bjorketun, M. E.; Herbst, K.; Bech, L.; Seger, B.; Pedersen, T.; Hansen, O.; Rossmeisl, J.; Dahl, S.; Norskov, J. K.; Chorkendorff, I. *J. Photonics Energy* **2012**, *2*.

(11) Hou, Y.; Abrams, B. L.; Vesborg, P. C. K.; Bjorketun, M. E.; Herbst, K.; Bech, L.; Setti, A. M.; Damsgaard, C. D.; Pedersen, T.; Hansen, O.; Rossmeisl, J.; Dahl, S.; Norskov, J. K.; Chorkendorff, I. *Nat. Mater.* **2011**, *10*, 434.
(12) Seo, S. W.; Park, S.; Jeong, H. Y.; Kim, S. H.; Sim, U.; Lee, C. W.; Nam, K. T.; Hong, K. S. *Chem. Commun.* **2012**, *48*, 10452.
(13) Cotton, F. A.; Dori, Z.; Llusar, R.; Schwotzer, W. *J. Am. Chem. Soc.* **1985**, *107*, 6734.
(14) Miller, W. K.; Gilbertson, J. D.; Leiva-Paredes, C.; Bernatis, P. R.; Weakley, T. J. R.; Lyon, D. K.; Tyler, D. R. *Inorg. Chem.* **2002**, *41*, 5453.
(15) Fedin, V. P.; Sokolov, M. N.; Mironov, Y. V.; Kolesov, B. A.; Tkachev, S. V.; Fedorov, V. Y. *Inorg. Chim. Acta* **1990**, *167*, 39.
(16) Cotton, F. A.; Kibala, P. A.; Matusz, M.; McCaleb, C. S.; Sandor, R. B. W. *Inorg. Chem.* **1989**, *28*, 2623.
(17) Sasaki, M.; Sakane, G.; Ouchi, T.; Shibahara, T. *J. Cluster Sci.* **1998**, *9*, 25.
(18) Cotton, F. A.; Wing, R. M.; Zimmerma, Ra *Inorg. Chem.* **1967**, *6*, 11.
(19) Fedin, V. P.; Gerascko, O. A.; Fedorov, V. E.; Slovokhotov, Y. L.; Struchkov, Y. T. *Izv. Sib. Otd. An. Khim.* **1988**, 64.
(20) Bublitz, D.; Preetz, W. *Z. Anorg. Allg. Chem.* **1996**, *622*, 1107.
(21) Binstead, R. A.; Jung, B.; Zuberbühler, A. D. *SPECFIT-32*; Spectrum Software Associates: Chapel Hill, NC, 2000.
(22) *CrysAlis*^{Pro}, version 171.35.11; Agilent Technologies: Santa Clara, CA, 2010.
(23) *CrysAlis*^{Pro}, version 171.36.24; Agilent Technologies: Santa Clara, CA, 2012.
(24) Clark, R. C.; Reid, J. S. *Acta Crystallogr., Sect. A* **1995**, *51*, 887.
(25) Sheldrick, G. M. *Acta Crystallogr., Sect. A* **2008**, *64*, 112.
(26) Dolomanov, O. V.; Bourhis, L. J.; Gildea, R. J.; Howard, J. A. K.; Puschmann, H. *J. Appl. Crystallogr.* **2009**, *42*, 339.
(27) Brandenburg, K.; Putz, H. *Diamond: Crystal and Molecular Structure Visualization*; Crystal Impact: Bonn, Germany, 2008.
(28) Llusar, R.; Vicent, C. In *Inorg. Chem. In Focus III (Chapter 7)*; Meyer, G., Naumann, D., Wesermann, L., Eds.; Wiley-VCH: Weinheim, Germany, 2006.
(29) Algarra, A. G.; Basallote, M. G.; Fernandez-Trujillo, M. J.; Guillamon, E.; Llusar, R.; Segarra, M. D.; Vicent, C. *Inorg. Chem.* **2007**, *46*, 7668.
(30) Basallote, M. G.; Jesus Fernandez-Trujillo, M.; Angel Pino-Charnorro, J.; Beltran, T. F.; Corao, C.; Llusar, R.; Sokolov, M.; Vicent, C. *Inorg. Chem.* **2012**, *51*, 6794.
(31) Avarvari, N.; Kiracki, K.; Llusar, R.; Polo, V.; Sorribes, I.; Vicent, C. *Inorg. Chem.* **2010**, *49*, 1894.
(32) Basallote, M. G.; Estevan, F.; Feliz, M.; Fernandez-Trujillo, M. J.; Hoyos, D. A.; Llusar, R.; Uriel, S.; Vicent, C. *Dalton Trans.* **2004**, 530.
(33) Basallote, M. G.; Feliz, M.; Fernandez-Trujillo, M. J.; Llusar, R.; Safont, V. S.; Uriel, S. *Chem.—Eur. J.* **2004**, *10*, 1463.
(34) Algarra, A. G.; Basallote, M. G.; Castillo, C. E.; Corao, C.; Llusar, R.; Fernandez-Trujillo, M. J.; Vicent, C. *Dalton Trans.* **2006**, 5725.
(35) Algarra, A. S. G.; Basallote, M. G.; Fernandez-Trujillo, M. J.; Llusar, R.; Safont, V. S.; Vicent, C. *Inorg. Chem.* **2006**, *45*, 5774.
(36) Feliz, M.; Guillamon, E.; Llusar, R.; Stiriba, S.-E.; Pérez Prieto, J.; Barberis, M. *Chem.—Eur. J.* **2006**, *2006*, 1486.
(37) Richens, D. T.; Pittet, P. A.; Merbach, A. E.; Humanes, M.; Lamprecht, G. J.; Ooi, B. L.; Sykes, A. G. *c* **1993**, 2305.
(38) Hernandez-Molina, R.; Sykes, A. G. *J. Chem. Soc., Dalton Trans.* **1999**, 3137.
(39) Hernandez-Molina, R.; Sokolov, M. N.; Sykes, A. G. *Acc. Chem. Res.* **2001**, *34*, 223.
(40) Algarra, A. G.; Basallote, M. G.; Feliz, M.; Fernandez-Trujillo, M. J.; Llusar, R.; Safont, V. S. *Chem.—Eur. J.* **2006**, *12*, 1413.
(41) Hernandez-Molina, R.; Sykes, A. G. *Coord. Chem. Rev.* **1999**, *187*, 291.
(42) Algarra, A. G.; Feliz, M.; Fernández-Trujillo, M. J.; Llusar, R.; Safont, V. S.; Vicent, C.; Basallote, M. G. *Chem.—Eur. J.* **2009**, *15*, 4582.
(43) Algarra, A. G.; Fernández-Trujillo, M. J.; Basallote, M. G. *Chem.—Eur. J.* **2012**, *18*, 5036.
(44) Algarra, A. G.; Sokolov, M.; González-Platas, J.; Fernández-Trujillo, M. J.; Basallote, M. G.; Hernández-Molina, R. *Inorg. Chem.* **2009**, *48*, 3639.
(45) Algarra, A. G.; Basallote, M. G.; Feliz, M.; Fernández-Trujillo, M. J.; Llusar, R.; Vicent, S. S. *Chem.—Eur. J.* **2010**, *16*, 1613.